MOLECULAR AND CELLULAR BIOLOGY, Dec. 1997, p. 7283–7294 Vol. 17, No. 12
0270-7306/97/$04.00+0

Fal1p Is an Essential DEAD-Box Protein Involved in 40S-Ribosomal-Subunit Biogenesis in *Saccharomyces cerevisiae*

DIETER KRESSLER,[1] JESÚS DE LA CRUZ,[1] MANUEL ROJO,[2] AND PATRICK LINDER[1]*

Département de Biochimie Médicale, Centre Médical Universitaire,[1] and Département de Biochimie, Sciences II,[2] Université de Genève, 1211 Geneva 4, Switzerland[1]

Received 2 July 1997/Returned for modification 31 July 1997/Accepted 3 September 1997

A previously uncharacterized *Saccharomyces cerevisiae* gene, *FAL1*, was found by sequence comparison as a homolog of the eukaryotic translation initiation factor 4A (eIF4A). Fal1p has 55% identity and 73% similarity on the amino acid level to yeast eIF4A, the prototype of ATP-dependent RNA helicases of the DEAD-box protein family. Although clearly grouped in the eIF4A subfamily, the essential Fal1p displays a different subcellular function and localization. An HA epitope-tagged Fal1p is localized predominantly in the nucleolus. Polysome analyses in a temperature-sensitive *fal1-1* mutant and a Fal1p-depleted strain reveal a decrease in the number of 40S ribosomal subunits. Furthermore, these strains are hypersensitive to the aminoglycoside antibiotics paromomycin and neomycin. Pulse-chase labeling of pre-rRNA and steady-state-level analysis of pre-rRNAs and mature rRNAs by Northern hybridization and primer extension in the Fal1p-depleted strain show that Fal1p is required for pre-rRNA processing at sites A_0, A_1, and A_2. Consequently, depletion of Fal1p leads to decreased 18S rRNA levels and to an overall deficit in 40S ribosomal subunits. Together, these results implicate Fal1p in the 18S rRNA maturation pathway rather than in translation initiation.

Proteins belonging to the DEAD-box family originate from a wide range of organisms from bacteria to humans (41, 61). They are involved in a variety of RNA metabolic processes, including translation initiation (51), pre-mRNA splicing (82), pre-rRNA processing (76), and RNA degradation (27). For some of these proteins, an ATP-dependent RNA helicase activity has been observed (24, 38, 57), but most are regarded as putative ATP-dependent RNA helicases. The family is characterized by a core region of around 300 to 350 amino acids that show strong homology to the translation initiation factor eIF4A, the prototype of the DEAD-box family proteins. The core region consists of eight motifs with strong sequence conservation, which classify the DEAD-box proteins in the superfamily II of nucleoside triphosphatases (22, 33). Until now, biochemical properties could be attributed to only four of the eight conserved motifs, as established for the mammalian translation initiation factor eIF4A: the ATPase A motif (AX_4GKT) is responsible for initial ATP binding; the ATPase B region (DEAD) is involved in ATP hydrolysis and couples ATP hydrolysis to helicase activity; the SAT region is important for RNA unwinding; and the HRIGRXXR region is involved in ATP hydrolysis-dependent RNA binding (50, 52). Sequence divergence within the DEAD box gives rise to the DEAH and the DEXH subgroups, which are more heterogeneous with respect to both sequence and biochemical function (18). Moreover, individual members of the family have distinct amino- and carboxy-terminal regions that vary in length (61). These additional regions and differences within the core region may confer substrate specificity, direct the protein to its subcellular localization, include RNA binding motifs, or bind to accessory proteins, which could by themselves carry out the aforementioned functions.

The RNA binding and bidirectional RNA helicase activity of eIF4A is stimulated by eIF4B (45, 57). During translation initiation, these two proteins are thought to remove secondary structures in the 5′ untranslated region of mRNAs. Such secondary structures impede 40S ribosome binding and movement (scanning process) (34). Thus, an RNA helicase activity is likely to be needed for translation initiation. Other DEAD-box proteins have not yet been biochemically studied to the same extent as eIF4A, and for most of them no ATP-dependent RNA helicase activity has been found. This could be because different DEAD-box proteins require specific substrates and/or accessory proteins to fulfill their duty. For other DEAD-box family proteins, an RNA-dependent ATPase activity has been found (19, 31, 64). Such an RNA-dependent ATPase activity may require a specific RNA, as shown for the *Escherichia coli* DbpA protein (19). Thus, most of the putative RNA helicases could exert their in vivo function by modulating the structure of an RNA and thereby regulating its function or its accessibility.

Yeast pre-rRNA processing involves a large number of *trans*-acting factors that are required for the proper maturation and assembly of the highly structured pre-rRNAs with proteins to form the ribosomal subunits (76). Even though putative RNA helicases have been reported to play a major role in this complex process, little is known about their precise involvement. The DEAD-box proteins Dbp4p, Rok1p, and Rrp3p are required for 18S rRNA processing (39, 49, 73), while Dbp3p, Drs1p, and Spb4p assist in the 25S rRNA maturation (55, 59, 83). A helicase activity could render the highly structured pre-rRNAs accessible for the endo- and exonucleolytic cleavage steps by local unwinding of RNA structures. Also, this activity could be required for the proper interaction of the pre-rRNA with small nucleolar RNAs (snoRNA), small nucleolar ribonucleoprotein particles (snoRNP), and ribosomal proteins during pre-rRNA processing and ribosomal subunit assembly (69, 76).

Here, we describe the isolation and functional analysis of the Fal1 (eIF4A-like) protein, which is the protein most closely related to the yeast translation initiation factor 4A (Tif1/2p) in the entire *Saccharomyces cerevisiae* genome. Fal1p is part of

* Corresponding author. Mailing address: Département de Biochimie Médicale, Centre Médical Universitaire, Université de Genève, 1 rue Michel-Servet, CH-1211 Geneva 4, Switzerland. Phone: 41 22 702 54 84. Fax: 41 22 702 55 02. E-mail: patrick.linder@medecine.unige.ch.

the eIF4A subfamily of DEAD-box proteins and is essential for cell viability. In contrast to the translation initiation function of eIF4A, Fal1p plays a role in 40S-ribosomal-subunit biogenesis and, more precisely, in the early pre-rRNA processing steps at sites A_0, A_1, and A_2 that are required for proper maturation of the 18S rRNA.

MATERIALS AND METHODS

Strains, media, and genetic methods. The *S. cerevisiae* strains in this study are derivatives of strain W303 (*MAT***a**/*MAT*α *ura3-1*/*ura3-1 ade2-1*/*ade2-1 his3-11,15*/*his3-11,15 leu2-3,112*/*leu2-3,112 trp1-1*/*trp1-1*) (67). YDK1 (*MAT***a**/*MAT*α *fal1*::kanMX4/*FAL1*) and YDK2 (*MAT***a**/*MAT*α *fal1*::HIS3MX6/*FAL1*) were obtained by transforming W303 with the LFH2-PCR product *fal1*::kanMX4 and *fal1*::HIS3MX6, respectively. YDK3 (*MAT***a**/*MAT*α *fal1*::kanMX4/*FAL1*) bears a *fal1*::kanMX4 disruption with the parental diploid being FY1679 (*MAT***a**/*MAT*α *ura3-52*/*ura3-52 his3*Δ*200*/*HIS3 leu2*Δ*1*/*LEU2 trp1*Δ*63*/*TRP1*) (84). YDK2-6B (*MAT***a** *fal1*::HIS3MX6) is a meiotic segregant of YDK2 that requires a plasmid-borne copy of *FAL1* for cell viability. SS13-3A [*MAT***a** *tif1*::*HIS3 tif2*::*ADE2* pSSC120(*CEN-LEU2*)-*tif1-1*] (62) and RCB1-1A (*MAT*α *stm1*::*ADE2*) (11) have been previously described. Genetic manipulations and the preparation of standard media were done by established procedures (4, 30). Antibiotic plates were prepared by adding the drugs from stock solutions into yeast extract-peptone-dextrose before pouring the plates. Cycloheximide, neomycin sulfate, and paromomycin sulfate were purchased from Sigma. Yeast cells were transformed by the lithium acetate method (20). One-step gene replacements were done by the method of Rothstein (56). For tetrad dissection, a Singer MSM micromanipulator was used.

***FAL1* disruption and cloning of its cognate ORF.** Deletion disruptions of *FAL1* were obtained by transformation of PCR-synthesized marker cassettes with long flanking homology regions (LFH-PCR) into the parental diploid strains (78, 80). Briefly, the template for the LFH1-PCR was genomic DNA prepared from FY1679. Separate PCRs were set up to obtain the 5′ long flanking homology region (including the start codon and pFA6a polylinker sequence at its 3′ end) and the 3′ long flanking homology region (including the stop codon and pFA6a polylinker sequence at its 5′ end). These LFH1-PCR products were then used as primers to amplify the kanMX4 or the HIS3MX6 heterologous marker modules from the *Eco*RV-linearized plasmid pFA6a-kanMX4 (80) or pFA6a-HIS3MX6 (79). The LFH2-PCR products were used to directly transform yeast. Selection for transformants was done either on YPD plates containing 200 mg of G418 (Gibco BRL) per liter or on synthetic dextrose minimal medium-His plates. Integration at the correct genomic locus was verified by analytical PCR and Southern blotting. The *fal1*::kanMX4 LFH2-PCR product was cloned into the *Eco*RV-restricted plasmid pUG7 (23) and subsequently subcloned into the *Not*I site of pRS416 (66) by release of the disruption cassette with *Not*I. To clone the cognate *FAL1* open reading frame (ORF) by gap repair (4), the kanMX4 marker was released from pRS416-*fal1*::kanMX4 by *Sph*I and *Pac*I. The gapped plasmid was gel purified (Gene Clean; Bio 101, Inc.) and then transformed into W303. Plasmid DNA of transformants was isolated (81), amplified in *E. coli*, and analyzed by restriction mapping. Gap-repaired plasmids (pRS416-*FAL1*) were transformed into YDK1, YDK2, and YDK3, and the complementation of the *fal1* null allele was tested by tetrad analysis. The plasmid pRS415-*FAL1* was constructed by cloning a 2.45-kb *Sac*II-*Bam*HI fragment from pRS416-*FAL1* into the *Sac*II-*Bam*HI-prepared vector pRS415.

The oligonucleotides used for the LFH-PCR were P5′ (5′AAT CAT GTT GAA TCA TGT CAT3′, starting 627 bp upstream of the *FAL1* start codon), P5′long (5′GGG GAT CCG TCG ACC TGC AGC G**CA TGT CTA ATG AGT TTT TTT TTT GTT TCT G**3′; the reverse complement of the *FAL1* start codon is in bold and underlined, and the *FAL1* 5′ upstream region is in bold), P3′long (5′AAA CGA GCT CGA ATT CAT CGA TGA TA**T AAA ATA TAG AGA ACA TAT ACC TAC AT**3′; the *FAL1* stop codon is in bold and underlined, and the *FAL1* 3′ downstream region is in bold), and P3′ (5′CAA GTA CAG ATT AGA AGA GAA3′, starting 624 bp downstream of the *FAL1* stop codon). For all PCRs, a mixture of Biotaq (Bioprobe) and Vent polymerase (New England Biolabs) was used.

Random PCR mutagenesis of *FAL1*. Temperature-sensitive *fal1* alleles were generated by random PCR mutagenesis, cotransformation of the PCR products with a gapped plasmid (48), and subsequent plasmid shuffling (8). Briefly, the template for the mutagenic PCR was the *Xho*I-restricted plasmid pRS416-*FAL1*. After PCR amplification with *Taq* polymerase (Gibco BRL) and primers P5′ and P3′, a 2.45-kb PCR product was obtained. PCR products (around 0.5 to 1 μg/transformation) were cotransformed with 20 ng of *Sph*I-*Pac*I-gapped, gel-purified pRS415-*FAL1* into strain YDK2-6B(pRS416-*FAL1*). A total of 2,500 transformants from five independent PCRs were obtained and replica plated on SD-Leu plates and 5-fluoroorotic acid (5-FOA) plates at both the permissive (30°C) and the nonpermissive (37°C) temperatures. Putative temperature-sensitive candidates were restreaked at both temperatures, and their plasmid DNA was extracted and amplified in *E. coli*. After retransformation into YDK2-6B (pRS416-*FAL1*) and subsequent plasmid shuffling, two temperature-sensitive *fal1* alleles were obtained.

***FAL1* HA epitope tagging and cloning under the control of a galactose-inducible promoter or its cognate promoter.** *FAL1* was PCR amplified (with Vent polymerase) with oligonucleotides introducing the restriction sites *Sal*I (5′GCA CGC GTC GAC **TCG TTT GAC AGA GAA GAA G**3′; the *Sal*I site is underlined, and the *FAL1* ORF homology, starting with the second codon, is in bold) and *Sph*I (5′GCA CAT GCA TGC **AGG AAA ACC AAA TGA GAA C**3′; the *Sph*I site is underlined, and the *FAL1* 3′ downstream homology region, starting 301 bp after the stop codon, is in bold). The 1.5-kb *Sal*I-*Sph*I-restricted PCR product was cloned into the *Sal*I-*Sph*I-cut YCplac111-based plasmid pAS24 (63). The resulting plasmid, pAS24-*FAL1*, contains a *GAL1-10* promoter, a start codon followed by a double HA tag, and the *FAL1* ORF. This construct was transformed into strain YDK2-6B(pRS416-*FAL1*), and segregation of the *URA3 FAL1*-harboring plasmid (5-FOA selection) resulted in strain YDK2-6B(pAS24-*FAL1*). We also refer to this strain as *GAL*::*FAL1*, the conditional *fal1* null strain, or, if grown in YPD medium, the Fal1p-depleted strain.

To express the epitope-tagged Fal1p from its cognate promoter at approximately wild-type levels, plasmid-borne *FAL1* (pRS415-*FAL1*) was also N-terminally HA tagged by fusion PCR (25). Briefly, two fragments with sequence overlap were generated in a first PCR series with the *Nde*I-restricted pRS416-*FAL1* as a template and the oligonucleotide couples 5′AGG GAT AGC CCG CAT AGT CAG GAA CAT CGT ATG GGT ATG C**CG ACA TGT CTA ATG AGT T**3′ (the *FAL1* ORF homology and 5′ upstream region are in bold, and the overlapping part of the double HA tag is underlined) and 5′AAC AGC TAT GAC CAT G3′ (reverse primer) and 5′TGA CTA TGC GGG CTA TCC CTA TGA CGT CCC GGA CTA TGC A**TC GTT TGA CAG AGA AGA AG**3′ (the *FAL1* ORF homology region is in bold, and the overlapping part of the double HA tag is underlined) and 5′GTA AAA CGA CGG CCA GT3′ (universal primer) as primers. These PCR products, together with the reverse and universal primers, were used for the fusion PCR. The final product was cloned as a *Sac*II-*Bam*HI fragment into the *Sac*II-*Sph*HI-restricted plasmid pRS415. This construct (pRS415-*HA-FAL1*) complemented the *fal1* null allele to the wild-type extent, and the HA-tagged Fal1p was detected by Western blotting as a band that migrated at the expected molecular mass of approximately 45 kDa.

Polysome analysis and total ribosomal subunit quantification. Polysome preparations were done by the method of Foiani et al. (15). Cultures were grown in YPD and harvested at an optical density at 600 nm (OD_{600}) between 0.5 and 1. Cycloheximide was added to a final concentration of 0.1 mg/ml immediately before harvesting. Cell extracts were prepared in 10 mM Tris-HCl (pH 7.5)–100 mM NaCl–30 mM $MgCl_2$ in the presence of 0.1 mg of cycloheximide per ml and 0.2 mg of heparin per ml. Extracts (8 absorption units at 260 nm [A_{260}]) were layered onto 11.2 ml of 7 to 50% linear sucrose gradients that were prepared in 50 mM Tris-acetate (pH 7.5)–50 mM NH_4Cl–12 mM $MgCl_2$–1 mM dithiothreitol. The gradients were centrifuged at 39,000 rpm in a Beckman SW41 rotor at 4°C for 2 h 45 min. Ribosomal-subunit quantification was done in low-Mg^{2+} gradients by the method of Foiani et al. (15). Cells were grown to an OD_{600} between 0.5 and 1 and harvested after a 20-min treatment with 1 mM NaN_3. Cycloheximide was omitted to produce a polysome runoff. The cells were washed and broken in 50 mM Tris-HCl (pH 7.4)–50 mM NaCl–1 mM dithiothreitol and processed as before, and 5 A_{260} units of extract was centrifuged as above on 7 to 50% linear sucrose gradients prepared in the same buffer. Gradient analysis was performed with an ISCO UV-6 gradient collector and continuously monitored at A_{254}.

Indirect immunofluorescence. Strains YDK2-6B(pRS415-*HA-FAL1*) and YDK2-6B(pRS415-*FAL1*) were grown to an OD_{600} of around 0.5 in YPD medium, and the cells were harvested by centrifugation. Yeast cells were prepared for immunofluorescence by standard procedures (53). DAPI (4′,6-diamidino-2-phenylindole dihydrochloride; purchased from Fluka) was used to stain DNA. Primary monoclonal mouse anti-HA antibodies (16B12; Berkeley Antibody Co.) at a dilution of 1/200 and secondary goat anti-mouse rhodamine-conjugated antibodies (Pierce) at a dilution of 1/200 were used to detect the HAFal1p. Polyclonal rabbit anti-Nop1p antibodies (obtained from E. C. Hurt, University of Heidelberg) at a dilution of 1/500 and secondary fluorescein-conjugated goat anti-rabbit antibodies (Pierce) at a dilution of 1/200 were used to detect the nucleolar protein Nop1p (71). Fluorescently labeled cells were inspected in a Zeiss Axiophot fluorescence microscope with the Plan-NEOFLUAR 100x/1.3 objective. Photographs were taken with Kodak TMAX p3200 and transferred to Kodak PhotoCD. For superimposition, pseudo-colors were assigned to the digitized micrographs and images were merged into a composite RGB image with Adobe Photoshop 3.0 and a Power Macintosh 7500/100 computer. Final figures were arranged with Microsoft PowerPoint 4.0 and printed on a Kodak Digital Science 8650 PS color printer.

Pulse-chase labeling of pre-rRNA. Cells of strains YDK2-6B(pAS24-*FAL1*) and YDK2-6B(pRS415-*FAL1*) were grown to an OD_{600} of around 1 in 40 ml of SD medium lacking methionine and concentrated in 1 ml of SD medium lacking methionine, and the pre-rRNA was pulse-labeled for 1 min with 250 μCi of [*methyl*-^{3}H]methionine (Amersham; specific activity, 70 to 85 Ci/mmol). The chase was initiated by diluting 250-μl aliquots of the pulse-labeled cells in 4 ml of SD medium containing 1 mg of methionine per ml. The cells were harvested after 0, 2, 5, and 15 min of chase, washed in ice-cold water, and frozen in liquid nitrogen. Total RNA was extracted by the acid-phenol method (4). The methyl group incorporation was measured by scintillation counting, and 20,000 cpm per RNA extract was loaded and resolved on 1.2% agarose–formaldehyde gels (75).

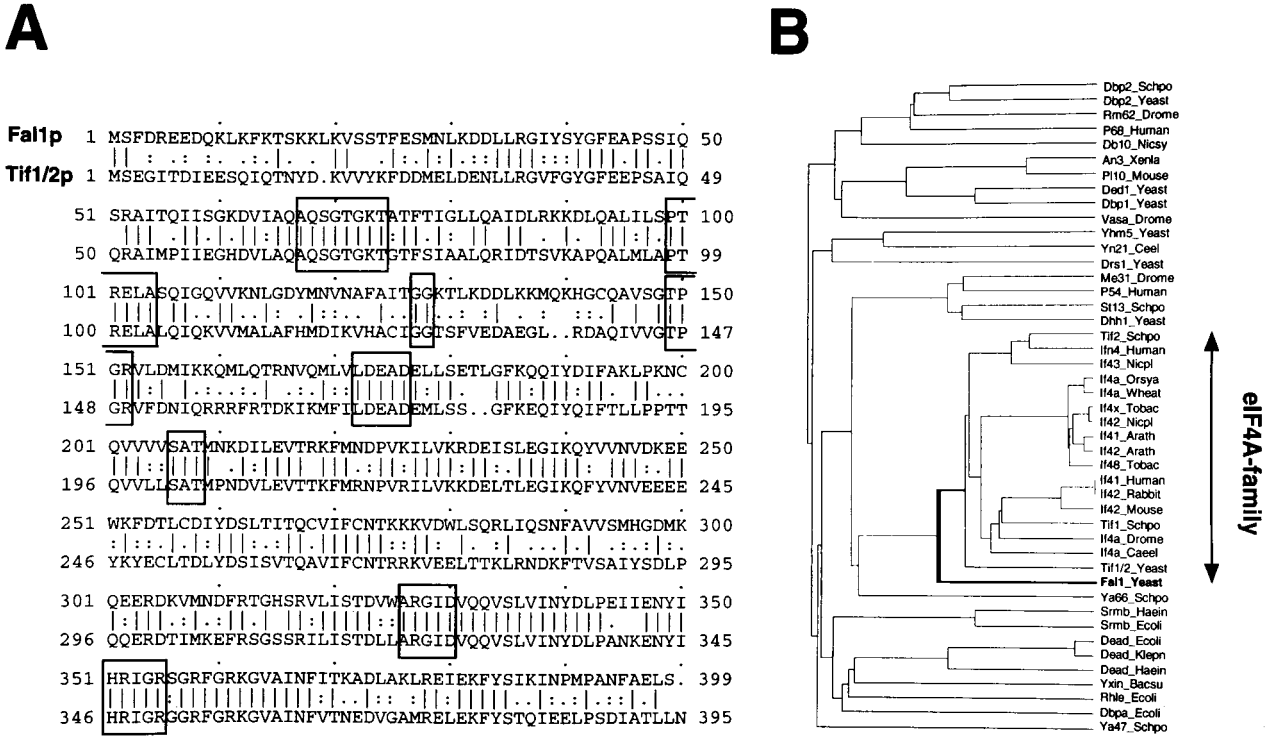

FIG. 1. Sequence analysis of Fal1p. (A) Predicted amino acid sequence of Fal1p and a gap alignment with the yeast eIF4A (Tif1/2p). Identities are indicated by vertical bars, and conservative substitutions are indicated by one or two dots. Boxes represent the eight conserved motifs characteristic of DEAD-box proteins. Alignment was performed by the GAP program of the Genetics Computer Group package. (B) Dendrogram analysis of DEAD-box proteins groups Fal1p within the eIF4A subfamily. The dendrogram was created by the PILEUP program. Sequence names are as referred to in SwissProt, except for Fal1_Yeast (SwissProt: IF4N_Yeast), Tif1/2_Yeast (IF4A_Yeast), Tif1_Schpo (IF4A_Schpo), and Tif2_Schpo (IF4N_Schpo).

RNA was transferred to Hybond-N^+ nylon membranes (Amersham) by capillary blotting. After being baked for 2 h at 80°C, the membranes were sprayed with EN^3HANCE (Du Pont), dried, and exposed to X-ray films for 4 days at −80°C with an intensifying screen.

Northern and primer extension analysis. Steady-state levels of pre-rRNAs were assessed by Northern and primer extension analyses. Oligonucleotides (numbered from 1 to 9 according to the scheme in Fig. 6A) $5'A_0$ (5′GGT CTC TCT GCT GCC GG3′), 18S (5′CAT GGC TTA ATC TTT GAG AC3′), D/A_2 (5′CGG TTT TAA TTG TCC TA3′), A_2/A_3 (5′TGT TAC CTC TGG GCC C3′), A_3/B_1 (5′AAT TTC CAG TTA CGA AAA TTC TTG3′), 5.8S (5′TTT CGC TGC GTT CTT CAT C3′), E/C_2 (5′GGC CAG CAA TTT CAA GTT A3′), C_1/C_2 (5′GAA CAT TGT TCG CCT AGA3′), and 25S (5′CTC CGC TTA TTG ATA TGC3′) were end labeled with 30 μCi of [γ-^{32}P]ATP (Amersham; specific activity, 5,000 Ci/mmol) by using T4 polynucleotide kinase (Appligene). Total RNA was extracted as above, and 5 μg was loaded and resolved on 1.2% agarose–formaldehyde gels. After the RNA was transferred to and immobilized on nylon membranes as above, it was stained with 0.02% (wt/vol) methylene blue in a 0.3 M sodium acetate (pH 5.5) solution. Prehybridization and hybridization were done in Church buffer (10). Washes were done in 2× SSC (1× SSC is 0.15 M NaCl plus 0.015 M sodium citrate)–0.5% sodium dodecyl sulfate and in 0.1× SSC–0.5% sodium dodecyl sulfate, and the membranes were exposed to X-ray films at −80°C with an intensifying screen. Low-molecular-weight RNAs were analyzed in 7% polyacrylamide–8 M urea gels by the method of Venema et al. (75). To assess the steady-state levels of snoRNAs, the following oligonucleotides were used: U3 (5′TTC GGT TTC TCA CTC TGG GGT AC3′), U14 (5′GGA ACC AGT CTT TCA TCA CC3′), snR10 (5′CCT TGC AAC GGT CCT CAT CCG GG3′), and snR30 (5′GAA GCG CCA TCT AGA TG3′).

Primer extension was done by the method of Venema and Tollervey (77). Oligonucleotides 2 and 7 were used as primers. To identify the positions of the primer extension stops, rDNA (the rDNA was PCR amplified from genomic DNA of W303 and cloned into pUC19) dideoxy sequencing reactions, generated with the above oligonucleotides, were run in parallel. Avian myeloblastosis virus reverse transcriptase and RNAguard were purchased from Pharmacia.

Miscellaneous. DNA manipulations were done by the method of Sambrook et al. (60) with *E. coli* DH10B for subcloning and amplification of plasmid DNA. For dideoxy sequencing, a T7 sequencing kit (Pharmacia) was used. DNA sequence comparisons were performed at the *Saccharomyces* Genome Database (Stanford) and at the National Center for Biotechnology Information. The Genetics Computer Group program from the Wisconsin package (version 8.1) was used for dendrogram analysis (PILEUP) and gap alignment (GAP). Phylogenetic trees were generated by the CLUSTAL W program (68). For prediction of the pI and the subcellular localization of proteins, the SwissProt program package was used (3). Crude yeast cell extracts were prepared and analyzed by Western blotting by standard procedures (4, 60). Monoclonal 16B12 and goat anti-mouse alkaline phosphatase-conjugated antibodies (Bio-Rad) were used as primary and secondary antibodies, respectively.

RESULTS

The eIF4A homolog Fal1p is essential for vegetative growth. With the release of the *S. cerevisiae* genome sequence, we performed a database search for homologs of eIF4A. This factor is encoded in yeast by the essential and duplicated *TIF1/2* genes (42). The most homologous ORF found (ORF YDR021W, chrIV; accession number Z49770) has 55% identity and 73% similarity to Tif1/2p on the amino acid level and has therefore been named *FAL1* (eIF4A-like).

The sequence alignment showed that all the characteristic DEAD-box protein motifs were conserved and that the homology regions extended throughout the two proteins (Fig. 1A). Dendrogram analysis of DEAD-box proteins with the PILEUP program established Fal1p as a member of the eIF4A subfamily (Fig. 1B). A phylogenetic tree generated with the CLUSTAL W program, by aligning only the core regions (from the A-motif to the HRIGR-motif), resulted in a similar and clear-cut (bootstrap value of 100) cogrouping of Fal1p and the eIF4A family of DEAD-box proteins (data not shown). In addition, the two proteins have similar lengths, with Fal1p being only 4 amino acids longer than Tif1/2p (399 versus 395 amino acids). Other non-eIF4A DEAD-box proteins have either N- or C-terminal extensions. Moreover, Fal1p was only

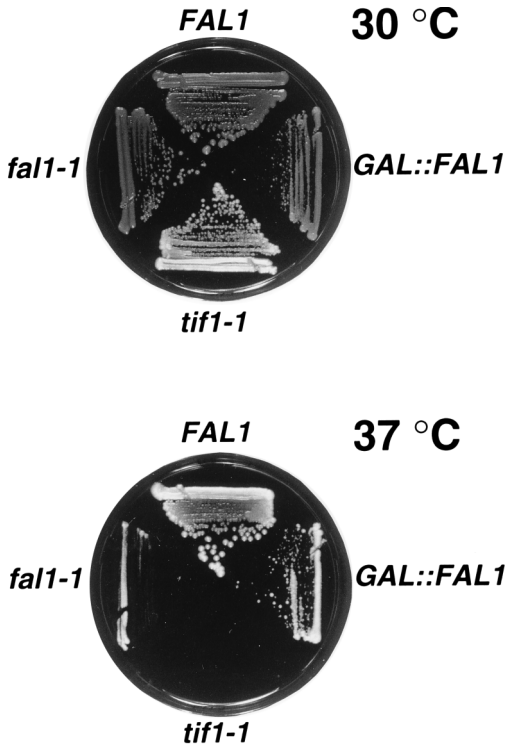

FIG. 2. Growth comparison of *fal1* affected strains. YDK2-6B(pRS416-*FAL1*) (*FAL1*), YDK2-6B(pRS415-*fal1-1*) (*fal1-1*), SS13-3A(pSSC120-*tif1-1*) (*tif1-1*), and YDK2-6B(pAS24-*FAL1*) (*GAL*::*FAL1*) were grown for 4 days at 30 or 37°C on YPD plates.

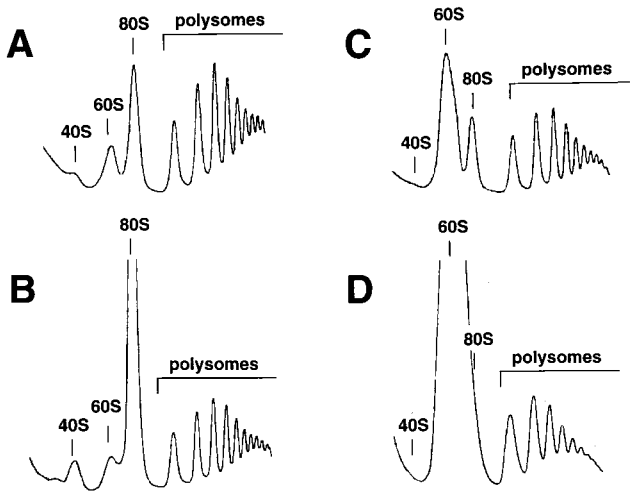

FIG. 3. The *fal1-1* mutation results in an accumulation of free 60S ribosomal subunits. (A to C) YDK2-6B(pRS416-*FAL1*) (A), SS13-3A(pSSC120-*tif1-1*) (B), YDK2-6B(pRS415-*fal1-1*) (C) were grown at 30°C. (D) YDK2-6B (pRS415-*fal1-1*) was grown at 30°C and shifted for 4 h to 37°C. Cells were grown in YPD and harvested at an OD_{600} of 0.8. Cell extracts were resolved in 7 to 50% sucrose gradients. The peaks of free 40S and 60S ribosomal subunits, 80S monosomes, and polysomes are indicated.

slightly less identical to human, mouse, or *Schizosaccharomyces pombe* eIF4A than was Tif1/2p.

However, further predictive data suggested that the two proteins might not be as similar as judged by the sequence homology. First, Fal1p has a much lower codon adaptation index (0.17 versus 0.75) and is therefore expected to have a lower expression level than Tif1/2p (65). Second, the calculated pIs differed dramatically, with Fal1p being basic (9.09) and Tif1/2p being acidic (5.02). Nevertheless, they have the same predicted cytoplasmic localization (SwissProt, Psort program) (3). Taken together, these data made us address whether Fal1p was a functional homolog of Tif1/2p, carrying out a similar role in translation initiation, or a protein involved in another RNA metabolic process, despite the substantial structural homology.

For this purpose, a *fal1* null allele was constructed. The entire *FAL1* ORF was replaced by either the kanMX4 or the HIS3MX6 marker modules. To this end, the LFH2-PCR products (see Materials and Methods) were used to directly transform the diploid strains W303 and FY1679. Correct integration at the genomic locus was verified by both analytical PCR and Southern blotting (data not shown). Subsequent tetrad analysis showed a 2:2 segregation of viable to nonviable spores, with all the viable progeny being *FAL1* and G418 sensitive or auxotrophic for histidine. The spores disrupted for *fal1* in the two different genetic backgrounds germinated, but cell division stopped after three to five generations.

The cognate *FAL1* ORF was cloned into pRS416 by gap repair and was shown to complement its null allele after transformation of the *FAL1*/*fal1*::HIS3MX6 heterozygote (YDK2) with pRS416-*FAL1* and subsequent sporulation and tetrad analysis [YDK2-6B(pRS416-*FAL1*) (Fig. 2)]. Furthermore, *FAL1* was required for vegetative growth as judged by the nongrowth of YDK2-6B (pRS416-*FAL1*) on 5-FOA-containing plates (data not shown). These results indicate that Fal1p is essential for cell viability.

Mutations in *FAL1* or in vivo depletion of Fal1p lead to a 40S-ribosomal-subunit deficiency. To further analyze the essential Fal1p function, two conditional systems for phenotypic analysis were established. First, temperature-sensitive *fal1* alleles were generated by random PCR mutagenesis (see Materials and Methods). Two mutant alleles, *fal1-1* and *fal1-3*, were obtained, and both displayed a slow-growth phenotype at 37°C, with *fal1-1* being the more severely affected allele (Fig. 2 for *fal1-1*; data not shown for *fal1-3*). The DNA sequences of wild-type *FAL1* (no changes to the released sequence) and *fal1-1* were determined. The nucleotide changes within the *fal1-1* allele and the corresponding predicted amino acid changes within Fal1-1p were as follows: T254C (Ile85Thr), A431G (Gln144Arg), T731C (Val244Ala), and T737C (Val246Ala). All these changes were within conserved amino acids between Fal1p and Tif1/2p. No systematic attempt has been made to determine whether all the predicted amino acid changes contribute to the temperature-sensitive phenotype.

Genetic evidence suggested that Fal1p and Tif1/2p did not have a common function in translation initiation. *TIF1* was not able to complement the *fal1* null or to suppress the *fal1-1* mutant when overexpressed. The *S. cerevisiae* eIF4B-gene (*STM1*/*TIF3*), a multicopy suppressor of a *tif1-1* mutant (11), failed to suppress *fal1-1* as well. Moreover, no synthetic lethality was observed for a Δ*stm1 fal1-1* strain, whereas Δ*stm1* and *tif1-1* are synthetically lethal (12). Finally, *FAL1* on a 2μm plasmid did not complement the *tif1/2* double null or suppress the *tif1-1* mutant.

Polysome analyses were performed to test whether Fal1p was implicated in translation. The two mutant strains (Fig. 3C for *fal1-1*, data not shown for *fal1-3*) had strongly aberrant profiles, but they were different from a classical translation initiation defect (as shown for *tif1-1* in Fig. 3B). In the *fal1-1* mutant, in contrast to the wild-type strain, the levels of free 40S subunits were decreased whereas the free 60S pool increased. This subunit imbalance was even more pronounced after shift-

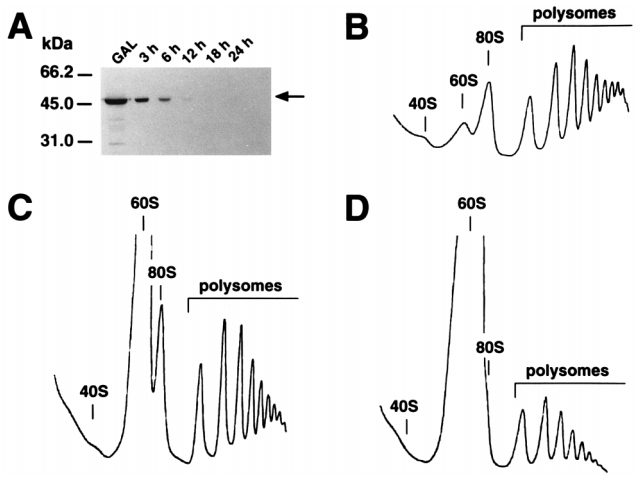

FIG. 4. Depletion of Fal1p results in an accumulation of free 60S ribosomal subunits. YDK2-6B(pAS24-*FAL1*) was grown in YPGal and shifted to YPD for up to 24 h. (A) Depletion of Fal1p. Cell extracts were prepared from samples harvested at the indicated times and assayed by Western blot analysis with the monoclonal mouse anti-HA antibody 16B12. Equal amounts of protein (70 μg) were loaded in each lane, as judged by Coomassie staining of gels or Ponceau red staining of the blots (data not shown). The Fal1p signal is indicated by an arrow. (B to D) Polysome analysis of YDK2-6B(pAS24-*FAL1*) after shifting the culture to YPD for 12 h (B), 18 h (C), or 24 h (D). Cell extracts were resolved in 7 to 50% sucrose gradients. The peaks of free 40S and 60S ribosomal subunits, 80S monosomes, and polysomes are indicated.

ing the *fal1-1* culture to 37°C for 4 h before preparing the crude cell extracts (Fig. 3D). In addition, the polysome content was lower at 37°C than at 30°C, probably accounting for the enhanced slow-growth phenotype. This 40S-ribosomal-subunit deficit was confirmed by quantification of total ribosomal subunits in polysome runoff and low-Mg^{2+} cell extracts. An A_{254} 60S-to-40S ratio of around 2 was observed for the wild-type strain at both 30 and 37°C; however, in the *fal1-1* mutant, this ratio increased to around 3 at 30°C and to more than 4 when *fal1-1* was shifted for 4 h to 37°C. Thus, polysome analysis indicated that Fal1p is implicated in 40S-ribosomal-subunit metabolism.

To confirm the 40S subunit deficiency, a different conditional system was established. The *FAL1* ORF was cloned under the control of the inducible *GAL1-10* promoter and HA tagged at its N terminus. This plasmid construct, pAS24-*FAL1*, complemented the *fal1* null (YDK2-6B) on galactose medium to the wild-type extent and resulted in a slow-growth phenotype on glucose medium at 30°C (Fig. 2). After YDK2-6B(pAS24-*FAL1*) was shifted from YPGal to YPD medium, the growth rate remained similar to that of a wild-type strain for the first 12 h, but then progressively decreased until a doubling time of 5 h was reached. Concomitant with the decrease in growth rate after 12 h in YPD medium, the cells started to be depleted for HA-Fal1p, as detected by Western blotting (Fig. 4A). When polysomes were analyzed after different time points, the same aberrant profiles were obtained with ongoing HA-Fal1p depletion as for the *fal1-1* mutant (Fig. 4B to D). Quantification of total ribosomal subunits showed a severe imbalance, which increased the A_{254} 60S-to-40S ratio to more than 6 for the 24-h depletion time point. These results indicated that mutations in *FAL1* and depletion of Fal1p lead to a similar 40S subunit deficit.

The *fal1-1* mutant and the Fal1p-depleted strain are hypersensitive to the aminoglycoside antibiotics paromomycin and neomycin. As the ribosomal subunits were imbalanced in the *fal1-1* mutant and in the Fal1p-depleted strain, we further characterized the 40S-subunit-defect phenotype by testing the sensitivity of these strains to different drugs known to interfere with protein synthesis: cycloheximide, paromomycin, and neomycin. The strains were grown overnight in YPD liquid medium and spotted in dilution series onto YPD plates containing different concentrations of the above-mentioned antibiotics. As a control, YPD plates without antibiotics were used.

TABLE 1. Sensitivity of *fal1* mutants to drugs impairing translation

Strain	Relevant genotype	Growth on[a]:			
		YPD	Par	Neo	Cyh
YDK2-6B(pRS416-*FAL1*)	Wild type	+	+	+	+
SS13-3A	*tif1-1*	+	−−	+/−	−
RCB1-1A	*stm1*::*ADE2*	+	−	+	−−
YDK2-6B(pRS415-*fal1-1*)	*fal1-1*	+	−−	−−	+
YDK2-6B(pAS24-*FAL1*)	*GAL*::*FAL1*	+	−−	−−	+

[a] Strains were spotted in three different dilutions on the different media, and growth was scored after 3 days at 30°C. +, normal growth; +/−, weak sensitivity; −, sensitivity; −−, hypersensitivity. Normal growth is defined for each strain as its growth rate on YPD. Abbreviations: YPD, rich medium containing no drugs; Par, YPD medium containing 2 mg of paromomycin per ml; Neo, YPD medium containing 5 mg of neomycin per ml; Cyh, YPD medium containing 0.1 μg of cycloheximide per ml.

Table 1 summarizes the results obtained. At the optimal drug concentrations, the wild-type strain was unaffected whereas the translation initiation factor mutants *tif1-1* (SS13-3A) and Δ*stm1* (RCB1-1A) were sensitive to paromomycin and cycloheximide. However, both the *fal1-1* mutant and the Fal1p-depleted strain were hypersensitive to paromomycin and neomycin, but their growth was not affected by cycloheximide. These results are consistent with a role of Fal1p in 40S-ribosomal-subunit production (see Discussion).

Fal1p localizes to the nucleolus. To distinguish between a cytoplasmic 40S-ribosomal-subunit defect and a nucleolar function of Fal1p in 40S-ribosomal-subunit biogenesis, the subcellular localization of Fal1p was analyzed by indirect immunofluorescence. For this purpose, *FAL1* was HA tagged at its N terminus by fusion PCR and cloned into pRS415 to express the epitope-tagged Fal1p from its cognate promoter at approximately wild-type levels (see Materials and Methods). This plasmid (pRS415-*HA-FAL1*) and a control plasmid (pRS415-*FAL1*), containing the untagged *FAL1* gene, were transformed into the strain YDK2-6B(pRS416-*FAL1*). Upon plasmid shuffling and subsequent restreaking on YPD, the Fal1 fusion protein complemented the *fal1* null allele to the wild-type extent at all temperatures tested (16, 30, and 37°C). In addition, Western analysis with an anti-HA antibody detected a single protein with the expected molecular mass of 45 kDa in a total-cell extract from a strain expressing the HA-tagged Fal1p [YDK2-6B(pRS415-*HA-FAL1*)] but not from a strain expressing the untagged Fal1p [YDK2-6B(pRS415-*FAL1*)] (data not shown). Then the two strains were grown in YPD to an OD_{600} of around 0.5, and the cells were processed for immunofluorescence. The HA-tagged protein was detected with anti-HA antibodies followed by decoration with goat anti-mouse rhodamine-conjugated antibodies (Fig. 5B). As controls, the nucleus was visualized by staining DNA with DAPI (Fig. 5C) and the nucleolus was visualized by the Nop1p signal, using anti-Nop1p in combination with fluorescien-conjugated antibodies (Fig. 5A). The fluorescence micrographs demonstrate that HA-Fal1p localizes to the nucleus (Fig. 5B), where it colocalizes with Nop1p in the nucleolus (Fig. 5D, overlap in yellow), and with chromatin DNA in the nucleoplasma (Fig.

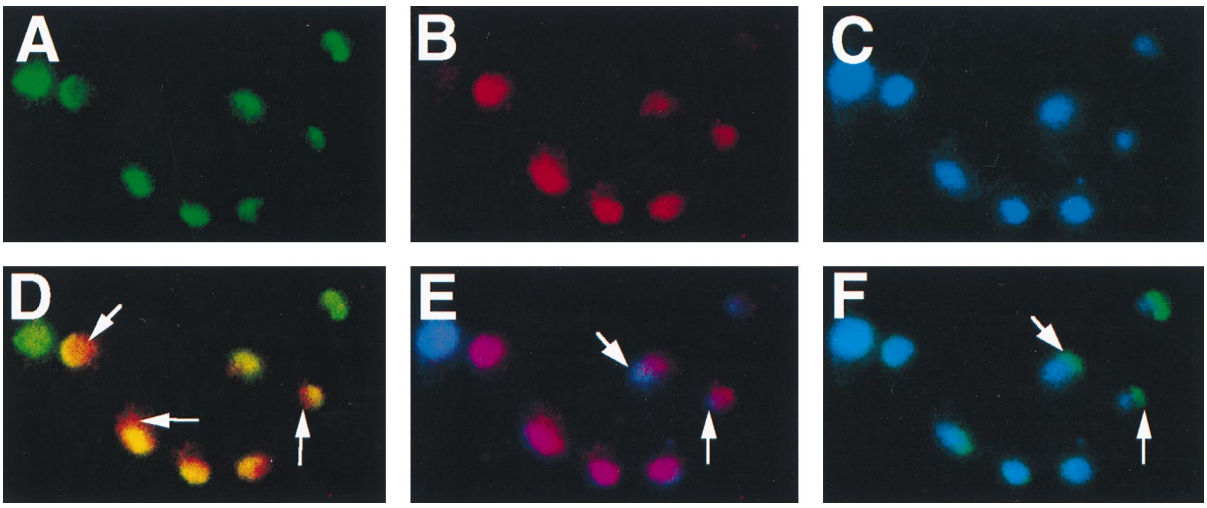

FIG. 5. Immunolocalization of HA-Fal1p. Indirect immunofluorescence was performed with cells expressing HA-Fal1p from the *FAL1* promoter [YDK2-6B(pRS415-*HA-FAL1*)]. (A) Nop1p was detected with polyclonal rabbit anti-Nop1p antibodies followed by decoration with a goat anti-rabbit fluorescein-conjugated antibody. (B) HA-Fal1p was detected by the monoclonal mouse anti-HA antibody 16B12 followed by decoration with a goat anti-mouse rhodamine-conjugated antibody. (C) Chromatin DNA was stained with DAPI. Pseudo-colors were assigned to the digitized micrographs (A to C), and images were merged. The overlapping distributions are revealed in yellow for HA-Fal1p and Nop1p colocalization (D), magenta for HA-Fal1p and chromatin DNA colocalization (E), and cyan for Nop1p and chromatin DNA colocalization (F). Arrows point to nuclear regions that are labeled for the single markers HA-Fal1p (D), chromatin DNA (E), and Nop1p (F).

5E, overlap in magenta). In contrast to Nop1p, HA-Fal1p was not restricted to the nucleolus (Fig. 5D, HA-Fal1p in red and marked with arrows) and also distributed to the nucleoplasma. In a significant number of cells, HA-Fal1p was not distributed throughout the entire nucleoplasma; hence, there were DAPI-stained areas where HA-Fal1p was not present (Fig. 5E, chromatin in blue and marked with arrows). However, the polarized distribution of HA-Fal1p within the nucleus was less pronounced than that of Nop1p, which often revealed the typical crescent or cap-like staining pattern of nucleolar proteins (Fig. 5A) and was mostly excluded from the DAPI-stained area (Fig. 5F, Nop1p in green and marked with arrows). Neither the nucleoplasmic nor the nucleolar Fal1p staining was present when YDK2-6B(pRS415-*FAL1*) was used for immunofluorescence (data not shown). The predominant localization of HA-Fal1p in the nucleolus, the specialized compartment for ribosome biosynthesis (44), indicated that Fal1p might be directly implicated in the biogenesis of 40S ribosomal subunits.

18S rRNA formation is impaired in the conditional *fal1* null strain. To study in more detail the involvement of Fal1p in 40S-ribosomal-subunit biogenesis, we analyzed the effects of Fal1p depletion on processing of pre-rRNA. In yeast, the rDNA operon is transcribed by the RNA polymerase I complex as a 35S precursor rRNA (Fig. 6A), which is processed into the mature 18S, 5.8S, and 25S rRNAs (reviewed in reference 76). Transcription, rRNA processing and modification, and ribosomal subunit assembly take place in the nucleolus (44). The 18S rRNA assembles into the 40S ribosomal subunit, whereas the 5.8S and the 25S rRNA (together with the RNA polymerase III-transcribed 5S rRNA) are part of the 60S subunits. The newly transcribed pre-rRNA undergoes different modifications including methylation of some of the nucleotides (32). The 60S subunit is completely matured within the nucleolus, whereas the final maturation of the 40S particle, including the processing of 20S to 18S rRNA, is completed in the cytoplasm (72, 76, 85). In the present model of the pre-rRNA processing pathway, the 35S pre-rRNA is cleaved to a 33S and then to a 32S pre-rRNA. The next cleavage generates the 20S pre-rRNA, which will give rise to the 18S rRNA and the $27SA_2$ pre-rRNA, which will be further processed to yield the 5.8S and the 25S rRNA (Fig. 6B).

To first investigate pre-rRNA processing, [*methyl*-^{3}H]methionine pulse-chase labeling experiments were carried out. For this purpose, YDK2-6B(pAS24-*FAL1*) and the wild-type control strain YDK2-6B(pRS415-*FAL1*) were grown as logarithmic cultures in YPGal, then for 18 h in YPD, and finally for another 12 h in SD medium lacking methionine until an OD_{600} of around 1 was achieved. At this time point, the Fal1p-depleted culture was doubling every 5 h, compared to every 2 h for the wild-type strain. The cells were pulse-labeled for 1 min and then chased for 2, 5, and 15 min with an excess of cold methionine. Comparison of the kinetics of pre-rRNA processing in the wild-type and the Fal1p-depleted strains revealed that processing of the 35S precursor is delayed in the Fal1p-depleted strain and that it is processed to a 27S pre-rRNA, an aberrant 23S rRNA species, and barely to the 20S precursor of the mature 18S rRNA (Fig. 7). However, processing of 27S to 25S seems not to be affected. Thus, impaired formation of the 20S pre-rRNA leads to a net decrease and delay in 18S rRNA production in the Fal1p-depleted strain.

To define the pre-rRNA processing steps that are affected upon Fal1p depletion, steady-state levels of pre-rRNAs were determined by Northern and primer extension analyses. Different oligonucleotides hybridizing to defined regions of the 35S pre-rRNA transcript were used to monitor specific processing intermediates in the *GAL*::*FAL1* strain (Fig. 6A). As seen in Fig. 8A, depletion of Fal1p resulted in a decrease in 18S rRNA compared to 25S rRNA steady-state levels. During probing with oligonucleotide 1 (Fig. 8B), hybridizing 5′ of the A_0 site, the *GAL*::*FAL1* strain accumulated, with ongoing depletion of Fal1p, the 35S pre-rRNA, and a 23S aberrant processing product. The accumulation of the 35S precursor was detected with all the other precursor-specific probes used. The aberrant product could also be detected with oligonucleotides 3 (Fig. 8C) and 4 (Fig. 8D) but not with oligonucleotide 5 (Fig. 8E), indicating that this rRNA molecule might extend from the 5′ end of the 5′ external transcribed spacer (ETS) to the A_3 site

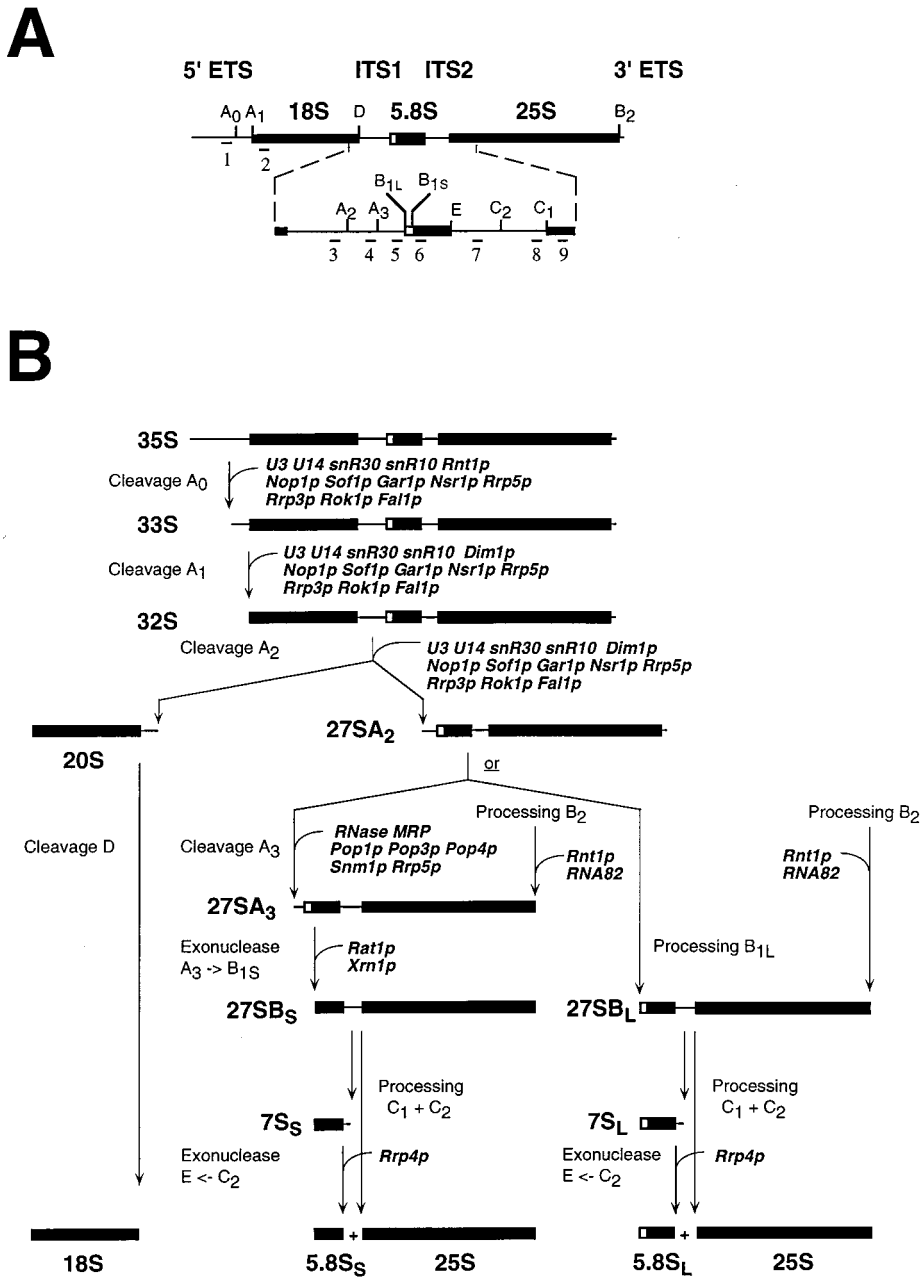

FIG. 6. Scheme of pre-rRNA processing in *S. cerevisiae*. (A) Structure and processing sites of the 35S pre-rRNA. The 35S operon contains the sequences for the mature 18S, 5.8S, and 25S rRNA that are separated by the two internal transcribed spacers ITS1 and ITS2. Two external transcribed spacers, the 5′ ETS and the 3′ ETS, are present at either end. The locations of the various probes (numbered from 1 to 9) used in this study are also indicated. Bars represent mature rRNA species, and lines represent the transcribed spacers. (B) Pre-rRNA processing pathway. The 35S pre-rRNA, the largest detectable precursor, is cleaved at site A_0 by the endonuclease Rnt1p (1), generating the 33S pre-rRNA. This molecule is subsequently processed at sites A_1 and A_2 to give rise to the 20S and $27SA_2$ precursors, resulting in the separation of the pre-rRNAs destined for the small and large ribosomal subunits. It is thought that the early pre-rRNA cleavages A_0 to A_2 are carried out by a large snoRNP complex (76), which is likely to be assisted by the putative ATP-dependent RNA helicases Fal1p (as described here), Rok1p (73), and Rrp3p (49). The final maturation of the 20S precursor takes place in the cytoplasm, where an endonucleolytic cleavage at site D yields the mature 18S rRNA. The $27SA_2$ precursor is processed by two alternative pathways that both lead to the formation of mature 5.8S and 25S rRNAs. In the major pathway, the $27SA_2$ precursor is cleaved at site A_3 and then quickly 5′-to-3′ exonucleolytically digested up to site B_{1S} to yield the $27SB_S$ precursor. A minor pathway involves direct cleavage of the $27SA_2$ molecule at site B_{1L}, producing the $27SB_L$ pre-rRNA. While processing at site B_1 is completed, the 3′ end of mature 25S rRNA is generated by processing at site B_2. The subsequent processing of both 27SB species appears to be identical. Cleavage at sites C_1 and C_2 releases the mature 25S rRNA and 7S pre-rRNAs, which undergo rapid 3′-to-5′ exonuclease digestion to the 3′ end of the mature 5.8S rRNA (site E). Note that impaired processing at sites A_0, A_1, and A_2, with a normal cleavage at site A_3, leads to the accumulation of a 23S aberrant processing intermediate (starting with the 5′ ETS and ending at the A_3 site) that will not be converted to the mature 18S rRNA. For reviews on pre-rRNA processing and *trans*-acting factors, see references 69 and 76.

and thus correspond to the previously described aberrant 23S processing product (76). Concomitant with Fal1p depletion, the amounts of the 32S pre-rRNA (Fig. 8B to F) and the 20S pre-rRNA (Fig. 8C), which is the direct precursor of the mature 18S rRNA, diminished. Consistent with the generation of the aberrant 23S rRNA species, we observed that the $27SA_2$ pre-rRNA was strongly depleted in the *GAL*::*FAL1* strain after 24 and 36 h in glucose (Fig. 8D and E). However, steady-state

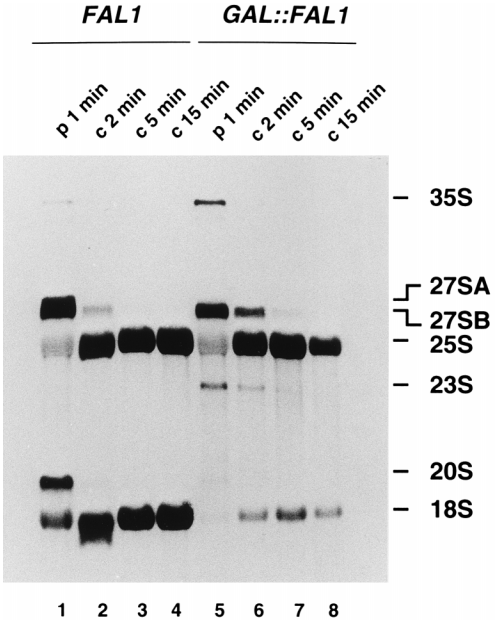

FIG. 7. Fal1p is required for the maturation of 18S rRNA. Cells were grown in SD medium without methionine, pulse-labeled for 1 min with [*methyl*-^{3}H]methionine, and then chased for 2, 5, and 15 min with an excess of unlabeled methionine. The wild-type control strain YDK2-6B(pRS415-*FAL1*) and strain YDK2-6B(pAS24-*FAL1*) were grown at 30°C in YPGal and then shifted to glucose-containing medium for 30 h before the pulse-labeling. A total of 20,000 cpm was loaded in each lane. The positions of the different pre-rRNAs and mature rRNAs are indicated.

levels of the 27SB intermediates were similar in wild-type and Fal1p-depleted cells, as observed when probing with the ITS2-specific oligonucleotides 7 (Fig. 8F) and 8 (data not shown). Moreover, when RNA samples were separated on acrylamide gels and subjected to Northern analysis with oligonucleotides 6 and 7, no differences in 7S and 5.8S rRNA levels were observed between wild-type and Fal1p-depleted cells. This Northern analysis data strongly implicated Fal1p as being essential for the early cleavage steps at sites A_0 to A_2. Normal steady-state levels of the snoRNAs U3, U14, snR10, and snR30, whose conditional mutants also display an A_0-to-A_2 processing block (26, 37, 47, 70), strengthened a direct involvement of Fal1p in pre-rRNA processing (data not shown). In addition, no *ACT1* pre-mRNA splicing defect could be detected in the *fal1-1* mutant or the Fal1p-depleted strain (data not shown).

Because Northern hybridization poorly detects the 33S or $27SA_3$ pre-rRNAs and does not distinguish between the $27SB_L$ and $27SB_S$ precursors, we assessed pre-rRNA and mature rRNA levels by primer extension. First, we confirmed that Fal1p depletion led to a net decrease in mature 18S rRNA levels, as shown by the primer extension stop at site A_1 (Fig. 9B). Moreover, the signal of the primer extension stop at site A_0 was significantly reduced (Fig. 9A). This delay in processing at site A_0, indicative of lower 33S pre-rRNA levels, is in agreement with the previous detection of the aberrant 23S species by Northern hybridization. Accordingly, the level of $27SA_2$, shown by the primer extension stop at site A_2, is strongly reduced (Fig. 9C). Furthermore, the levels of $27SA_3$, $27SB_L$, and $27SB_S$, as shown by the primer extension stops at sites A_3, B_{1L}, and B_{1S}, respectively, were similar to the wild-type situation (Fig. 9C). Finally, processing at all sites tested was correct at the nucleotide level during the time course of Fal1p depletion.

Altogether, these results indicate that Fal1p is required for the early pre-rRNA processing steps (A_0 to A_2) leading to the formation of the mature 18S rRNA. This interpretation is consistent with the other experimental findings, such as the aberrant polysome profiles (excess of free 60S over 40S subunits) and the sensitivity to aminoglycoside antibiotics in *fal1*-affected strains, as well as the predominantly nucleolar localization of the HA-Fal1p.

DISCUSSION

To learn more about the function of yeast eIF4A in translation initiation in particular and of DEAD-box proteins in general, we performed a systematic database search for proteins homologous to Tif1/2p. By this approach, one previously uncharacterized protein was found with 55% identity and 73% similarity to Tif1/2p, and we have named the corresponding gene *FAL1*. Gene disruption showed the *FAL1* gene to be essential for cell viability. Since a double disruption of *TIF1/2* is lethal, it was quite unlikely that Fal1p would carry out a redundant translation initiation function. Indeed, genetic analyses strongly suggested that Fal1p is not involved in translation initiation.

Several experimental findings indicate that Fal1p plays a role in 40S-ribosomal-subunit biogenesis.

(i) Polysome analysis and total ribosomal subunit quantification in both a *fal1-1* strain and a conditional *fal1* null strain reveal, rather than an accumulation of free 80S ribosomes, as observed for translation initiation mutants (5, 11), a ribosomal subunit imbalance leading to an excess of free 60S over free 40S. Such profiles have been described for mutants with mutations in 40S ribosomal proteins (2, 16) and for genes implicated in 40S-ribosomal-subunit biogenesis (14, 36).

(ii) Both the *fal1-1* and the conditional *fal1* null strain are hypersensitive to paromomycin and neomycin, but their growth is not affected by cycloheximide. Sensitivity to paromomycin and other aminoglycoside antibiotics has been observed for the *nsr1* null allele (36) and some *rps18a* and *rps18b* mutants (16). Nsr1p is required for 18S rRNA maturation and the proper maintenance of steady-state levels of 40S ribosomal subunits. *RPS18A* and *RPS18B* are duplicated genes encoding the 40S-ribosomal-subunit protein S18. Paromomycin is known to be an efficient suppressor of nonsense or missense mutations in *E. coli* and yeast. Defined mutations within the 18S rRNA exhibit an antisuppressor effect and confer increased resistance to paromomycin, and one of these mutations leads also to neomycin sensitivity (9). These data suggest that the 18S rRNA, in the context of the 40S ribosomal subunit, is the target of the antibiotics paromomycin and neomycin. On the other hand, a specific mutation in the 60S-ribosomal-subunit protein L29 confers resistance to cycloheximide (17). Thus, it is not surprising that only the aminoglycoside antibiotics lead to a synthetic enhancement in *fal1* affected strains.

(iii) In agreement with a role of Fal1p in 40S-ribosomal-subunit biogenesis, we could localize the N-terminally HA-tagged Fal1p predominantly, but not exclusively, in the yeast nucleolus. Although, we cannot exclude that Fal1p could have an additional, non-pre-rRNA-processing nuclear function, similar localization patterns have been previously observed for other proteins involved in pre-rRNA processing (58, 73). However, weak overexpression of HA-Fal1p from the *CEN*-plasmid construct or partial loss of function due to tagging might also account for the nonexclusive nucleolar localization. Interestingly, Fal1p is predicted to be cytoplasmic, and it lacks a consensus nuclear localization signal. This finding may indicate that Fal1p carries an as yet unknown signal sequence for nu-

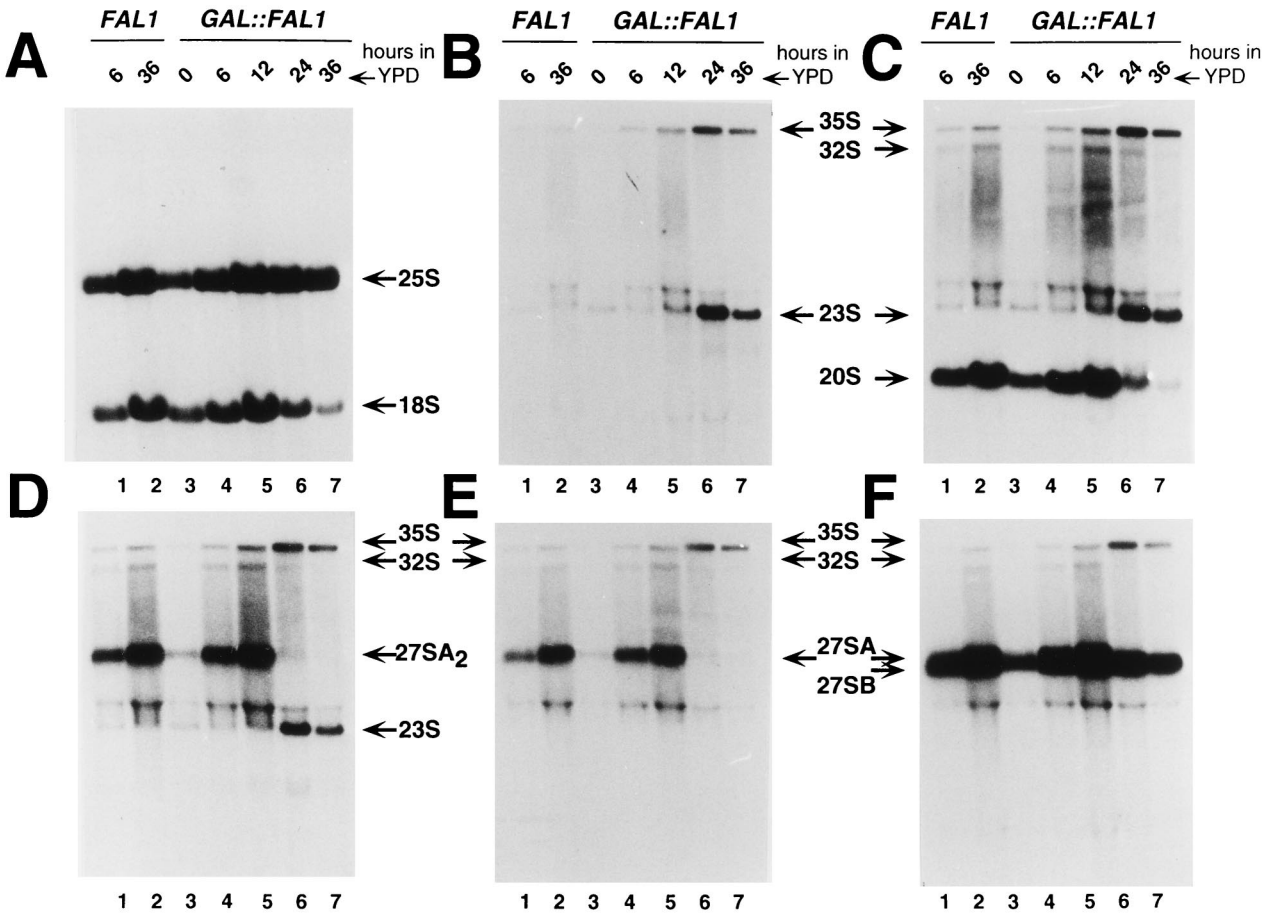

FIG. 8. Effect of Fal1p depletion on steady-state levels of pre-rRNA and mature rRNA species. Strains YDK2-6B(pRS416-*FAL1*) (*FAL1* [lanes 1 and 2]) and YDK2-6B(pAS24-*FAL1*) (*GAL*::*FAL1* [lanes 3 to 7]) were grown in YPGal and shifted to YPD. The cells were harvested at the different indicated times, and total RNA was extracted and subjected to Northern analysis. Note that the same filter was consecutively hybridized with all the different probes indicated in Fig. 6A. (A) Oligonucleotides 2 and 9, base pairing to sequences within the mature 18S and 25S rRNA, respectively. (B) Oligonucleotide 1 in the 5′ ETS. (C) Oligonucleotide 3 in ITS1 between sites D and A_2. (D) Oligonucleotide 4 in ITS1 between sites A_2 and A_3. (E) Oligonucleotide 5 in ITS1 downstream of site A_3. (F) Oligonucleotide 7 in ITS2 between sites E and C_2. The positions of the different pre-rRNAs and mature rRNAs are indicated.

clear targeting or that it is imported into the nucleus by binding to a nuclear-targeted protein in the cytoplasm.

(iv) Finally, our results indicate that Fal1p plays a role in 18S rRNA maturation. Pulse-chase labeling of rRNA with [*methyl*-^{3}H]methionine in both the *fal1-1* mutant (data not shown) and the conditional *fal1* null strain (Fig. 7) confirmed the ribosomal subunit imbalance at the level of the ratio between matured 25S to 18S rRNA. Furthermore, this metabolic labeling showed that the processing from 20S to 18S rRNA was not affected but that there was already a depletion of the 20S pre-rRNA species. Such a processing defect, leading to decreased amounts of 20S and 18S rRNA, has been previously observed for other mutant strains. These strains are conditional for snoRNAs (U3, U14, snR30, and snR10) (26, 37, 47, 70), some nucleolar proteins (Gar1p, Sof1p, Dim1p, Nop1p, and Rrp5p) (21, 28, 35, 71, 77), and two putative ATP-dependent RNA helicases (Rrp3p and Rok1p) (49, 73).

To confirm the 18S rRNA processing defect and to rule out an 18S rRNA methylation deficiency, we investigated the pre-rRNA steady-state levels by Northern and primer extension analyses. According to the current model (Fig. 6B), the early cleavages at the processing sites A_0, A_1, and A_2 are endonucleolytic, concomitant, but not obligatorily coupled, and they are carried out in a large snoRNP complex comprising the aforementioned snoRNAs and nucleolar proteins (76). Cleavage at site A_0 can be carried out in vitro by Rnt1p, an RNase III-like endonuclease (1), suggesting that, at least for the A_0 cleavage, the snoRNP complex plays only an accessory role rather than a catalytic one. A defect in the A_0-to-A_2 cleavages, with a correct A_3 cleavage, will lead to an accumulation of an aberrant pre-rRNA species, designated 23S (76), and to a normal $27SA_3$ precursor, which can be subsequently processed to the mature 5.8S and 25S rRNAs. However, the aberrant 23S intermediate cannot be processed to the mature 18S rRNA. Consequently, the early processing defects will lead to a depletion of the 20S and 18S rRNA species while 5.8S and 25S rRNA processing remain unaffected.

Northern hybridizations showed that Fal1p depletion had all the characteristics of a specific A_0-to-A_2 processing-site inhibition: accumulation of the 35S pre-rRNA and the aberrant 23S dead-end product and depletion of the 32S, $27SA_2$, 20S, and 18S rRNA species. Furthermore, Fal1p is not simply required for the synthesis or the stability of snoRNAs, which are important for proper A_0-to-A_2 processing, since the steady-state levels of U3, U14, snR30, and snR10 were not affected by the Fal1p depletion.

Primer extension experiments confirmed the Northern hybridization results and additionally indicated that the 33S pre-

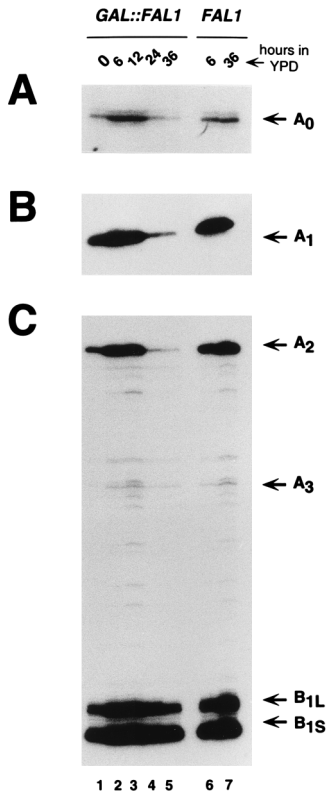

FIG. 9. Primer extension analysis of pre-rRNA. Fal1p depletion inhibits pre-rRNA processing at sites A_0, A_1, and A_2. The same RNA samples as for the Northern analysis in Fig. 8 were used. (A and B) Primer extension with oligonucleotide 2, priming within the mature 18S rRNA region, to examine the processing sites A_0 (A) and A_1 (B). (C) Primer extension from oligonucleotide 7 within ITS2 through the processing sites B_{1S}, B_{1L}, A_3, and A_2. The positions of the primer extension stops corresponding to the different pre-rRNA species and the mature 18S rRNA are indicated.

rRNA steady-state levels were also decreased, as shown by the primer extension stop at site A_0. Processing at the A_0 site seems to be significantly inhibited but not as strongly as cleavage at the sites A_1 and A_2. Still, inhibition of processing at the A_0 site upon depletion of Fal1p is more pronounced than upon depletion of Rok1p (73), Rrp5p (77), Gar1p, U14, snR30, and snR10 (6), but it is not as drastic as that found upon mutation or depletion of Rnt1p (1), U3 (26), and the U3-snoRNP-complex components Nop1p and Sof1p (6). However, accumulation of the 35S pre-rRNA and the aberrant 23S rRNA species in the Fal1p-depleted strain, as shown by Northern hybridization, indicates that cleavage at the site A_0 is significantly inhibited. In contrast, genetic depletion of Dim1p, an 18S rRNA dimethylase that is required solely for the processing at sites A_1 and A_2 (35), or certain *cis* mutations around the A_1 site (74) lead to an accumulation of the 33S pre-rRNA and a different, aberrant rRNA species, termed 22S, that extends from the A_0 site to the A_3 site.

By incorporating all the experimental evidence, we propose that Fal1p, a putative ATP-dependent RNA helicase, is involved in the maturation of the 18S rRNA by assisting in the processing at cleavage sites A_0, A_1, and A_2. Considering its presumed RNA helicase activity, a Fal1p-dependent, localized unwinding activity at the A_0 to A_2 cleavage sites may be required for the endonucleolytic processing reactions at these sites. There is evidence that such an RNA modulation model is reasonable. For example, the *E. coli* RhlB protein, a member of the DEAD-box family, was found within the RNA degradosome that contains both the endonucleolytic cleavage activity of RNase E and the 3′-to-5′ exonucleolytic degradation activity of polynucleotide phosphorylase (54). Another recent report of an exoribonuclease-associated helicase (Suv3p) has come from the characterization of a 3′-to-5′ exoribonuclease complex found in the yeast mitochondria (43). However, a role for an RNA helicase in modulating secondary structures that might otherwise block ribonucleolytic activities has to be shown in the case of pre-rRNA processing. In addition, the snoRNAs U3 and U14 base pair with extended regions within the 5′ ETS and the mature 18S rRNA (7, 40). Thus, it is also possible that Fal1p plays a role in the association-dissociation reactions between one of the aforementioned essential snoRNAs and their target sequences in the pre-rRNA. Finally, we cannot exclude that Fal1p could play a role in 40S-ribosomal-subunit assembly. Extensive rearrangements between pre-rRNA and ribosomal proteins are expected to occur during the assembly reactions, which may require the involvement of different *trans*-acting factors, including RNA helicases. In fact, evidence suggests that ribosomal subunit biogenesis and pre-rRNA processing are tightly linked and concomitant (76). For example, mutations in ribosomal proteins can lead to a feedback inhibition of pre-rRNA processing as a result of a ribosomal assembly defect (13, 46). Thus, impaired pre-rRNA processing could be a consequence of improper assembly of the 40S ribosomal subunit in the absence of Fal1p.

Fal1p is not the only DEAD-box protein described to be involved in pre-rRNA processing in yeast. Dbp3p (83), Drs1p (55), and Spb4p (59) are required for 25S rRNA processing, and Dbp4p (39), Rok1p (73), and Rrp3p (49) are required for proper 18S rRNA maturation. Since Fal1p, Rok1p, and Rrp3p have been described to be essential for cell viability, it is unlikely that they carry out redundant functions. In addition, comparison of the primary amino acid sequence between Fal1p and Dbp4p, Rok1p, or Rrp3p shows substantial differences and the last three proteins have also N- and C-terminal extensions that contain predicted nuclear localization signals and might be involved in conferring substrate specificity.

Since eIF4A and Fal1p are the shortest DEAD-box proteins in the databases, they could form the minimal structural domain needed for helicase activity. Since mammalian eIF4A requires eIF4B for efficient in vitro RNA-binding and helicase activity (29, 57), it is reasonable to speculate that the functional differences between eIF4A and Fal1p are mediated by specific partner proteins. Further experiments are required to elucidate the domains of eIF4A and Fal1p that make them function in the two different RNA metabolic processes. In addition, the nomenclature of the eIF4A homologs emerging from different organisms should be reconsidered. Since the highly similar Tif1/2p and Fal1p are exclusively implicated in translation initiation or pre-rRNA processing, eIF4A-like proteins should be termed "translation initiation factor 4A" only if such a function has been clearly demonstrated.

ACKNOWLEDGMENTS

We thank M. Rekik for technical assistance, A. Schmidt and M. N. Hall (University of Basel) for plasmid pAS24, U. Güldener and J. H. Hegemann (University of Giessen) for plasmid pUG7, and E. C. Hurt (University of Heidelberg) for the kind gift of the anti-Nop1p antibodies. We are grateful to A.-L. Veuthey for CLUSTAL analysis. We are indebted to B. Dichtl (University of Edinburgh) for providing a pre-rRNA processing scheme. We thank J. Venema and members of our laboratory for fruitful discussions, and we thank I. Iost, K. Tanner, and J. Venema for critical reading of the manuscript.

J.C. acknowledges a fellowship from the Spanish government (Ministerio de Educación y Ciencia) and support from Sandoz-Stiftung and

Ciba-Geigy Jubiläums-Stiftung. This work was supported by a grant from the Swiss National Science Foundation to P.L. (31-43321.95).

REFERENCES

1. **Abou Elela, S., H. Igel, and M. Ares, Jr.** 1996. RNase III cleaves eukaryotic preribosomal RNA at a U3 snoRNP-dependent site. Cell **85:**115–124.
2. **Abovich, N., L. Gritz, L. Tung, and M. Rosbash.** 1985. Effect of *RP51* gene dosage alterations on ribosome synthesis in *Saccharomyces cerevisiae*. Mol. Cell. Biol. **5:**3429–3435.
3. **Appel, R. D., A. Bairoch, and D. F. Hochstrasser.** 1994. A new generation of information retrieval tools for biologists: the example of the ExPASy WWW server. Trends Biochem. Sci. **19:**258–260.
4. **Ausubel, F. M., R. Brent, R. E. Kingston, D. D. Moore, J. G. Seidman, J. A. Smith, and K. Struhl.** 1994. Current protocols in molecular biology, vol. 2. John Wiley & Sons, Inc., New York, N.Y.
5. **Barnes, C. A., R. A. Singer, and G. C. Johnston.** 1993. Yeast *prt1* mutations alter heat-shock gene expression through transcript fragmentation. EMBO J. **12:**3323–3332.
6. **Beltrame, M., Y. Henry, and D. Tollervey.** 1994. Mutational analysis of an essential binding site for the U3 snoRNA in the 5′ external transcribed spacer of yeast pre-rRNA. Nucleic Acids Res. **22:**5139–5147.
7. **Beltrame, M., and D. Tollervey.** 1995. Base pairing between U3 and the pre-ribosomal RNA is required for 18S rRNA synthesis. EMBO J. **14:**4350–4356.
8. **Boeke, J. D., J. Trueheart, G. Natsoulis, and G. R. Fink.** 1987. 5-Fluoroorotic acid as a selective agent in yeast molecular genetics. Methods Enzymol. **154:**164–175.
9. **Chernoff, Y. O., A. Vincent, and S. W. Liebman.** 1994. Mutations in eukaryotic 18S ribosomal RNA affect translational fidelity and resistance to aminoglycoside antibiotics. EMBO J. **13:**906–913.
10. **Church, G. M., and W. Gilbert.** 1984. Genomic sequencing. Proc. Natl. Acad. Sci. USA **81:**1991–1995.
11. **Coppolecchia, R., P. Buser, A. Stotz, and P. Linder.** 1993. A new yeast translation initiation factor suppresses a mutation in the eIF-4A RNA helicase. EMBO J. **12:**4005–4011.
12. **de la Cruz, J., I. Iost, D. Kressler, and P. Linder.** 1997. The p20 and Ded1 proteins have antagonistic roles in eIF4E-dependent translation in *Saccharomyces cerevisiae*. Proc. Natl. Acad. Sci. USA **94:**5201–5206.
13. **Deshmukh, M., Y.-F. Tsay, A. G. Paulovich, and J. L. Woolford, Jr.** 1993. Yeast ribosomal protein L1 is required for the stability of newly synthesized 5S rRNA and the assembly of 60S ribosomal subunits. Mol. Cell. Biol. **13:**2835–2845.
14. **Finley, D., B. Bartel, and A. Varshavsky.** 1989. The tails of ubiquitin precursors are ribosomal proteins whose fusion to ubiquitin facilitates ribosome biogenesis. Nature **338:**394–401.
15. **Foiani, M., A. M. Cigan, C. J. Paddon, S. Harashima, and A. G. Hinnebusch.** 1991. GCD2, a translational repressor of the *GCN4* gene, has a general function in the initiation of protein synthesis in *Saccharomyces cerevisiae*. Mol. Cell. Biol. **11:**3203–3216.
16. **Folley, L. S., and T. D. Fox.** 1994. Reduced dosage of genes encoding ribosomal protein S18 suppresses a mitochondrial initiation codon mutation in *Saccharomyces cerevisiae*. Genetics **137:**369–379.
17. **Fried, H. M., and J. R. Warner.** 1982. Molecular cloning and analysis of yeast gene for cycloheximide resistance and ribosomal protein L29. Nucleic Acids Res. **10:**3133–3147.
18. **Fuller-Pace, F. V.** 1994. RNA helicases: modulators of RNA structure. Trends Cell Biol. **4:**271–274.
19. **Fuller-Pace, F. V., S. M. Nicol, A. D. Reid, and D. P. Lane.** 1993. DbpA: a DEAD box protein specifically activated by 23S rRNA. EMBO J. **12:**3619–3626.
20. **Gietz, D., A. St. Jean, R. A. Woods, and R. H. Schiestl.** 1992. Improved method for high efficiency transformation of intact yeast cells. Nucleic Acids Res. **20:**1425.
21. **Girard, J.-P., H. Lehtonen, M. Caizergues-Ferrer, F. Amalric, D. Tollervey, and B. Lapeyre.** 1992. GAR1 is an essential small nucleolar RNP protein required for pre-rRNA processing in yeast. EMBO J. **11:**673–682.
22. **Gorbalenya, A. E., E. V. Koonin, A. P. Donchenko, and V. M. Blinov.** 1989. Two related superfamilies of putative helicases involved in replication, recombination, repair and expression of DNA and RNA genomes. Nucleic Acids Res. **17:**4713–4730.
23. **Güldener, U., and J. H. Hegemann.** Unpublished data.
24. **Hirling, H., M. Scheffner, T. Restle, and H. Stahl.** 1989. RNA helicase activity associated with the human p68 protein. Nature **339:**562–564.
25. **Ho, S. N., H. D. Hunt, R. M. Horton, J. K. Pullen, and L. R. Pease.** 1989. Site-directed mutagenesis by overlap extension using the polymerase chain reaction. Gene **77:**51–59.
26. **Hughes, J. M. X., and M. Ares, Jr.** 1991. Depletion of U3 small nucleolar RNA inhibits cleavage in the 5′ external transcribed spacer of yeast preribosomal RNA and impairs formation of 18S ribosomal RNA. EMBO J. **10:**4231–4239.
27. **Jacobs Anderson, J. S., and R. Parker.** 1996. RNA turnover: the helicase story unwinds. Curr. Biol. **6:**780–782.
28. **Jansen, R., D. Tollervey, and E. C. Hurt.** 1993. A U3 snoRNP protein with homology to splicing factor PRP4 and Gβ domains is required for ribosomal RNA processing. EMBO J. **12:**2549–2558.
29. **Jaramillo, M., K. Browning, T. E. Dever, S. Blum, H. Trachsel, W. C. Merrick, J. M. Ravel, and N. Sonenberg.** 1990. Translation initiation factors that function as RNA helicases from mammals, plants and yeast. Biochim. Biophys. Acta **1050:**134–139.
30. **Kaiser, C., S. Michaelis, and A. Mitchell.** 1994. Methods in yeast genetics: a Cold Spring Harbor Laboratory course manual. Cold Spring Harbor Laboratory Press, Cold Spring Harbor, N.Y.
31. **Kim, S.-H., J. Smith, A. Claude, and R.-J. Lin.** 1992. The purified yeast pre-mRNA splicing factor PRP2 is an RNA-dependent NTPase. EMBO J. **11:**2319–2326.
32. **Klootwijk, J., and R. J. Planta.** 1989. Isolation and characterization of yeast ribosomal RNA precursors and preribosomes. Methods Enzymol. **180:**96–109.
33. **Koonin, E. V.** 1991. Similarities in RNA helicases. Nature **352:**290.
34. **Kozak, M.** 1989. The scanning model for translation: an update. J. Cell Biol. **108:**229–241.
35. **Lafontaine, D., J. Vandenhaute, and D. Tollervey.** 1995. The 18S rRNA dimethylase Dim1p is required for pre-ribosomal RNA processing in yeast. Genes Dev. **9:**2470–2481.
36. **Lee, W.-C., D. Zabetakis, and T. Mélèse.** 1992. NSR1 is required for pre-rRNA processing and for the proper maintenance of steady-state levels of ribosomal subunits. Mol. Cell. Biol. **12:**3865–3871.
37. **Li, H. V., J. Zagorski, and M. J. Fournier.** 1990. Depletion of U14 small nuclear RNA (snR128) disrupts production of 18S rRNA in *Saccharomyces cerevisiae*. Mol. Cell. Biol. **10:**1145–1152.
38. **Liang, L., W. Diehl-Jones, and P. Lasko.** 1994. Localization of vasa protein to the *Drosophila* pole plasm is independent of its RNA-binding and helicase activities. Development **120:**1201–1211.
39. **Liang, W.-Q., J. A. Clark, and M. J. Fournier.** 1997. The rRNA-processing function of the yeast U14 small nucleolar RNA can be rescued by a conserved RNA helicase-like protein. Mol. Cell. Biol. **17:**4124–4132.
40. **Liang, W.-Q., and M. J. Fournier.** 1995. U14 base-pairs with 18S rRNA: a novel snoRNA interaction required for rRNA processing. Genes Dev. **9:**2433–2443.
41. **Linder, P., P. F. Lasko, M. Ashburner, P. Leroy, P. J. Nielsen, K. Nishi, J. Schnier, and P. P. Slonimski.** 1989. Birth of the D-E-A-D box. Nature **337:**121–122.
42. **Linder, P., and P. P. Slonimski.** 1989. An essential yeast protein, encoded by duplicated genes *TIF1* and *TIF2* and homologous to the mammalian translation initiation factor eIF-4A, can suppress a mitochondrial missense mutation. Proc. Natl. Acad. Sci. USA **86:**2286–2290.
43. **Margossian, S. P., H. Li, H. P. Zassenhaus, and R. A. Butow.** 1996. The DExH box protein Suv3p is a component of a yeast mitochondrial 3′-to-5′ exoribonuclease that suppresses group I intron toxicity. Cell **84:**199–209.
44. **Mélèse, T., and Z. Xue.** 1995. The nucleolus: an organelle formed by the act of building a ribosome. Curr. Opin. Cell Biol. **7:**319–324.
45. **Méthot, N., A. Pause, J. W. B. Hershey, and N. Sonenberg.** 1994. The translation initiation factor eIF-4B contains an RNA-binding region that is distinct and independent from its ribonucleoprotein consensus sequence. Mol. Cell. Biol. **14:**2307–2316.
46. **Moritz, M., B. A. Pulaski, and J. L. Woolford, Jr.** 1991. Assembly of 60S ribosomal subunits is perturbed in temperature-sensitive yeast mutants defective in ribosomal protein L16. Mol. Cell. Biol. **11:**5681–5692.
47. **Morrissey, J. P., and D. Tollervey.** 1993. Yeast snR30 is a small nucleolar RNA required for 18S rRNA synthesis. Mol. Cell. Biol. **13:**2469–2477.
48. **Muhlrad, D., R. Hunter, and R. Parker.** 1992. A rapid method for localized mutagenesis of yeast genes. Yeast **8:**79–82.
49. **O'Day, C. L., F. Chavanikamannil, and J. Abelson.** 1996. 18S rRNA processing requires the RNA helicase-like protein Rrp3. Nucleic Acids Res. **24:**3201–3207.
50. **Pause, A., N. Méthot, and N. Sonenberg.** 1993. The HRIGRXXR region of the DEAD box RNA helicase eukaryotic translation initiation factor 4A is required for RNA binding and ATP hydrolysis. Mol. Cell. Biol. **13:**6789–6798.
51. **Pause, A., and N. Sonenberg.** 1993. Helicases and RNA unwinding in translation. Curr. Opin. Struct. Biol. **3:**953–959.
52. **Pause, A., and N. Sonenberg.** 1992. Mutational analysis of a DEAD box RNA helicase: the mammalian translation initiation factor eIF-4A. EMBO J. **11:**2643–2654.
53. **Pringle, J. R., A. E. M. Adams, D. G. Drubin, and B. K. Haarer.** 1991. Immunofluorescence methods for yeast, p. 565–602. *In* C. Guthrie and G. R. Fink (ed.), Guide to yeast genetics and molecular biology. Academic Press, Inc., San Diego.
54. **Py, B., C. F. Higgins, H. M. Krisch, and A. J. Carpousis.** 1996. A DEAD-box RNA helicase in the *Escherichia coli* RNA degradosome. Nature **381:**169–172.
55. **Ripmaster, T. L., G. P. Vaughn, and J. L. Woolford, Jr.** 1992. A putative ATP-dependent RNA helicase involved in *Saccharomyces cerevisiae* ribosome assembly. Proc. Natl. Acad. Sci. USA **89:**11131–11135.

56. **Rothstein, R. J.** 1983. One-step gene disruption in yeast. Methods Enzymol. **101:**202–211.
57. **Rozen, F., I. Edery, K. Meerovitch, T. E. Dever, W. C. Merrick, and N. Sonenberg.** 1990. Bidirectional RNA helicase activity of eucaryotic translation initiation factors 4A and 4F. Mol. Cell. Biol. **10:**1134–1144.
58. **Russell, I. D., and D. Tollervey.** 1992. NOP3 is an essential yeast protein which is required for pre-rRNA processing. J. Cell Biol. **119:**737–747.
59. **Sachs, A. B., and R. W. Davis.** 1990. Translation initiation and ribosomal biogenesis: involvement of a putative rRNA helicase and RPL46. Science **247:**1077–1079.
60. **Sambrook, J., E. F. Fritsch, and T. Maniatis.** 1989. Molecular cloning: a laboratory manual, 2nd ed. Cold Spring Harbor Laboratory Press, Cold Spring Harbor, N.Y.
61. **Schmid, S. R., and P. Linder.** 1992. D-E-A-D protein family of putative RNA helicases. Mol. Microbiol. **6:**283–292.
62. **Schmid, S. R., and P. Linder.** 1991. Translation initiation factor 4A from *Saccharomyces cerevisiae*: analysis of residues conserved in the D-E-A-D family of RNA helicases. Mol. Cell. Biol. **11:**3463–3471.
63. **Schmidt, A., M. Bickle, T. Beck, and M. N. Hall.** 1997. The yeast phosphatidylinositol kinase homolog TOR2 activates RHO1 and RHO2 via the exchange factor ROM2. Cell **88:**531–542.
64. **Schwer, B., and C. Guthrie.** 1991. PRP16 is an RNA-dependent ATPase that interacts transiently with the spliceosome. Nature **349:**494–499.
65. **Sharp, P. M., E. Cowe, D. G. Higgins, D. C. Shields, K. H. Wolfe, and F. Wright.** 1988. Codon usage patterns in *Escherichia coli*, *Bacillus subtilis*, *Saccharomyces cerevisiae*, *Schizosaccharomyces pombe*, *Drosophila melanogaster* and *Homo sapiens*: a review of the considerable within-species diversity. Nucleic Acids Res. **16:**8207–8211.
66. **Sikorski, R. S., and P. Hieter.** 1989. A system of shuttle vectors and yeast host strains designed for efficient manipulation of DNA in *Saccharomyces cerevisiae*. Genetics **122:**19–27.
67. **Thomas, B. J., and R. Rothstein.** 1989. Elevated recombination rates in transcriptionally active DNA. Cell **56:**619–630.
68. **Thompson, J. D., D. G. Higgins, and T. J. Gibson.** 1994. CLUSTAL W: improving the sensitivity of progressive multiple sequence alignment through sequence weighting, position-specific gap penalties and weight matrix choice. Nucleic Acids Res. **22:**4673–4680.
69. **Tollervey, D.** 1996. *trans*-acting factors in ribosome synthesis. Exp. Cell Res. **229:**226–232.
70. **Tollervey, D.** 1987. A yeast small nuclear RNA is required for normal processing of pre-ribosomal RNA. EMBO J. **6:**4169–4175.
71. **Tollervey, D., H. Lehtonen, M. Carmo-Fonseca, and E. C. Hurt.** 1991. The small nucleolar RNP protein NOP1 (fibrillarin) is required for pre-rRNA processing in yeast. EMBO J. **10:**573–583.
72. **Udem, S. A., and J. R. Warner.** 1973. The cytoplasmic maturation of a ribosomal precursor ribonucleic acid in yeast. J. Biol. Chem. **248:**1412–1416.
73. **Venema, J., C. Bousquet-Antonelli, J.-P. Gelugne, M. Caizergues-Ferrer, and D. Tollervey.** 1997. Rok1p is a putative RNA helicase required for rRNA processing. Mol. Cell. Biol. **17:**3398–3407.
74. **Venema, J., Y. Henry, and D. Tollervey.** 1995. Two distinct recognition signals define the site of endonucleolytic cleavage at the 5′-end of yeast 18S rRNA. EMBO J. **14:**4883–4892.
75. **Venema, J., R. J. Planta, and H. A. Raué.** *In vivo* mutational analysis of ribosomal RNA in *Saccharomyces cerevisiae. In* R. Martin (ed.), Protein synthesis: methods and protocols, in press. Humana Press, Totowa, N.J.
76. **Venema, J., and D. Tollervey.** 1995. Processing of pre-ribosomal RNA in *Saccharomyces cerevisiae*. Yeast **11:**1629–1650.
77. **Venema, J., and D. Tollervey.** 1996. *RRP5* is required for formation of both 18S and 5.8S rRNA in yeast. EMBO J. **15:**5701–5714.
78. **Wach, A.** 1996. PCR-synthesis of marker cassettes with long flanking homology regions for gene disruptions in *S. cerevisiae*. Yeast **12:**259–265.
79. **Wach, A., A. Brachat, C. Alberti-Segui, C. Rebischung, and P. Philippsen.** 1997. Heterologous *HIS3* marker and GFP reporter modules for PCR-targeting in *Saccharomyces cerevisiae*. Yeast **13:**1065–1075.
80. **Wach, A., A. Brachat, R. Pöhlmann, and P. Philippsen.** 1994. New heterologous modules for classical or PCR-based gene disruptions in *Saccharomyces cerevisiae*. Yeast **10:**1793–1808.
81. **Ward, A.** 1990. Single-step purification of shuttle vectors from yeast for high frequency back-transformation into *E. coli*. Nucleic Acids Res. **18:**5319.
82. **Wassarman, D. A., and J. A. Steitz.** 1991. Alive with DEAD proteins. Nature **349:**463–464.
83. **Weaver, P. L., C. Sun, and T.-H. Chang.** 1997. Dbp3p, a putative RNA helicase in *Saccharomyces cerevisiae*, is required for efficient pre-rRNA processing predominantly at site A_3. Mol. Cell. Biol. **17:**1354–1365.
84. **Winston, F., C. Dollard, and S. L. Ricupero-Hovasse.** 1995. Construction of a set of convenient *Saccharomyces cerevisiae* strains that are isogenic to S288C. Yeast **11:**53–55.
85. **Woolford, J. L., Jr., and J. R. Warner.** 1991. The ribosome and its synthesis, p. 587–626. *In* J. R. Broach, J. R. Pringle, and E. W. Jones (ed.), The molecular and cellular biology of the yeast *Saccharomyces*: genome dynamics, protein synthesis, and energetics, vol. 1. Cold Spring Harbor Laboratory Press, Cold Spring Harbor, N.Y.